Enhancement of mass anisotropy in an electron - phonon coupled model close to a Van Hove singularity

1997 J. Phys.: Condens. Matter 9 10195

(http://iopscience.iop.org/0953-8984/9/46/017)

J. Phys.: Condens. Matter **9** (1997) 10195–10202. Printed in the UK PII: S0953-8984(97)86251-0

Enhancement of mass anisotropy in an electron–phonon coupled model close to a Van Hove singularity

S Caprara and V Del Prete

Dipartimento di Fisica, Università degli Studi di Roma, P le Aldo Moro, 00185 Roma, Italy

Received 23 July 1997, in final form 24 September 1997

Abstract. We investigate the effect of electronic mass renormalization due to the coupling of electrons to an Einstein phonon in the presence of a Van Hove singularity in the density of states, resulting from a saddle point in the bare electronic spectrum. We show that an enhancement of mass anisotropy is produced in a wide region of parameters of our model.

The problem of the effect of a Van Hove singularity (VHS) in the density of states (DOS), close to the Fermi level, on the physical properties of an electronic system has been the object of a great interest.

Even before the discovery of high-T_c superconductors (HTSC), the presence of a VHS was considered as one of the possible factors which could contribute to increase the superconducting critical temperature T_c, within a BCS scheme [1]. The discovery of high-T_c superconductors (HTSC) has stimulated a new interest in the Van Hove scenario [2], to account for both the superconducting and anomalous metallic properties of these materials.

In a two-dimensional system the presence of a logarithmic VHS in the DOS is a topological consequence of the lattice periodicity [3], which manifests itself in the presence of saddle points in the electronic band structure. High-resolution experiments of angle-resolved photoemission (ARPES) performed on various classes of HTSC indeed reveal the presence of extended anisotropic saddle points [4–7] at the coordinates $(0, \pm\pi)$, $(\pm\pi, 0)$ in the two-dimensional Brillouin zone: the flattening of the band spreads over a large portion of k-space moving from $(0, \pi)$ along the y direction; however, when $\underline{k}$ varies along the x direction the quasi-particle peak moves rapidly towards higher binding energies, until it reaches the Fermi level. The width and the strong anisotropy of the saddle point are two properties that cannot be described to this extent by LDA calculations. Moreover these extended saddle points yield a divergence in the DOS which is stronger than the logarithmic VHS; this may have important consequences on the value of T_c [5], as well as on the transport properties of the system, due to the enhancement of phase space allowed for scattering processes.

In this paper we address a much simpler issue than explaining the complexity of the band structure of the cuprates [8]. Within a simple model, we show that in the presence of a saddle point in the electronic spectrum, the coupling of electrons to phonons may lead to an enhancement of mass anisotropy. In particular we consider as a perturbative term to a lattice-electron bare Hamiltonian the coupling to an Einstein phonon

$$\omega_0 \sum_q a_q^\dagger a_q + \sum_{k,q,\sigma} g_q (a_{-q}^\dagger + a_q)(c_{k+q}^\dagger c_k - \langle c_{k+q}^\dagger c_k \rangle) \tag{1}$$

0953-8984/97/4610195+08$19.50

where $a_q^\dagger$ creates a dispersionless Einstein phonon of a constant frequency ω_0 and momentum q, and the coupling constant is given by

$$g_q = g \qquad \text{when } |q_x|, |q_y| < q_c$$
$$g_q = 0 \qquad \text{when } |q_x|, |q_y| > q_c$$

where q_c is a cut-off for the momentum transfer. We have subtracted the average value of $c_{k+q}^\dagger c_k$ to eliminate the Hartree contribution to the self-energy.

The electron–phonon interaction can give an isotropic mass enhancement when the bare electronic band is parabolic [9]. We show that starting with a realistic two-dimensional-lattice band, the mass renormalization around the saddle point is anisotropic. Indeed the main mechanism for mass renormalization in [9] is the presence of a jump in the imaginary part of the self-energy at the phonon threshold ω_0, and the consequent divergence of the real part of the self-energy. This in turn produces the pinning of a quasi-particle peak with strong mass renormalization. Our main argument is that, close to a saddle point in the electronic spectrum, the above mechanism is more active in one direction in k-space, giving rise to the aforementioned anisotropic mass enhancement.

Although our result may not have a direct relevance to HTSC, we still refer to these systems to choose the parameters of the model and to compare our final conclusions with the experimental results. To reproduce the experimentally observed shape of the Fermi surface of the cuprates the following electronic band is usually considered

$$\xi(\underline{k}) = -2t\left[\cos(k_x) + \cos(k_y) + \alpha\cos(k_x)\cos(k_y)\right] - \mu \tag{2}$$

$\alpha = 2t'/t$ being a measure of the strength of the next-to-nearest-neighbours hopping parameter t'. In all our calculations we consider a unitary lattice spacing and all the energies are measured from the chemical potential μ. At the bottom of the band, corresponding to the point $\underline{k} = (0, 0)$, the dispersion (2), expanded to the second order, is parabolic with isotropic effective masses

$$\xi(\underline{k}) \simeq E_0 + \frac{k_x^2 + k_y^2}{2m_0} \tag{3}$$

where $E_0 = -2t(2+\alpha) - \mu$ and $1/m_0 = 2t(1+\alpha)$. As we previously remarked, within the Migdal approximation, a self-consistent expression for the self-energy may be found analitically for the model (1) in the case of a parabolic band [9]. When $|\xi(\underline{k})| \ll \omega_0$ the quasi-particle dispersion may be written as

$$\tilde{\xi}(\underline{k}) \simeq \frac{\xi(\underline{k})}{1+\lambda}$$
$$\lambda = -\left.\frac{\partial \Re\Sigma}{\partial\varepsilon}\right|_{\varepsilon=0} = \frac{g^2 N(0)}{\omega_0} \tag{4}$$

where $N(0)$ is the DOS, which is actually constant in two dimensions for the parabolic band (3), and $\lambda < 1$ in a weak-coupling regime, where vertex corrections are negligible. A second order expansion of (2) around the saddle point $(0, \pi)$, gives a hyperbolic band

$$\xi(\underline{k}) = E_0 + \frac{k_x^2}{2m_x} - \frac{k_y^2}{2m_y} \tag{5}$$

where $E_0 = 2\alpha t - \mu$, $1/m_x = 2t(1-\alpha)$, $1/m_y = 2t(1+\alpha)$, and k_y is the momentum in the y direction measured from the point $(0, \pi)$. As we want to investigate the effect of the electron–phonon interaction on the electronic effective mass close to the saddle point we perform a lowest-order perturbative calculation of the electron self-energy within the

Migdal approximation, assuming (5) as the bare band. We choose our parameters to obtain a small value for λ in (4), close to the parabolic bottom of the band, but there is no reason to assume that vertex corrections may be neglected close to the saddle point [10]. Nevertheless the spirit of our paper is to determine the contribution of the Fock diagram to the mass renormalization in a region around the saddle point, choosing our parameters with respect to the weak-coupling condition $\lambda < 1$ in a region of k-space close to the origin of coordinates.

The second-order self-energy, in this case, is given by

$$\Sigma(\underline{k}, \varepsilon_\nu) = T \sum_{\underline{q}} g_q^2 \sum_n \mathcal{D}(\underline{q}, \omega_n)\mathcal{G}(\underline{k} + \underline{q}, \varepsilon_\nu + \omega_n)$$

$\mathcal{D}(\underline{q}, \omega_n)$ and $\mathcal{G}(\underline{k}, \varepsilon_\nu)$ are the bare phononic and electronic propagators in the Matsubara formalism. After performing the summation on the Matsubara frequencies and extending this to real frequencies we obtain

$$\Sigma(\underline{k}, \varepsilon) = \sum_{\underline{q}} g_q^2 \left[\frac{b(\omega_0) + f(\xi(\underline{k} + \underline{q}))}{\xi(\underline{k} + \underline{q}) - \omega_0 - \varepsilon - \mathrm{i}\delta} + \frac{b(-\omega_0) + f(\xi(\underline{k} + \underline{q}))}{\xi(\underline{k} + \underline{q}) + \omega_0 - \varepsilon - \mathrm{i}\delta} \right]$$

where $f(z)$ is the Fermi function, $b(z)$ is the Bose function and assuming $b(z - \mathrm{i}\varepsilon_\nu) = -f(z)$. In the limit of zero temperature we obtain for the imaginary part of Σ

$$\begin{aligned} \Im\Sigma(\underline{k}, \varepsilon) = {} & \pi \sum_{\underline{q}} g_q^2 [1 - \vartheta(\varepsilon + \omega_0)] \delta(\xi(\underline{k} + \underline{q}) - \omega_0 - \varepsilon) \\ & - \pi \sum_{\underline{q}} g_q^2 \vartheta(\varepsilon - \omega_0) \delta(\varepsilon - \omega_0 - \xi(\underline{k} + \underline{q})). \end{aligned} \tag{6}$$

The presence of the ϑ functions in (6) imposes a threshold at $\pm\omega_0$. In addition, from (6) we notice that in the limit $q_c \to \infty$ we may change the sum variable $\underline{q} \to \underline{q} + \underline{k}$ making evident that in this case the self-energy does not depend on $\underline{k}$. This independence is only approximate, when the cut-off is finite, for $|\underline{k}|/q_c \ll 1$, i.e. in a large portion of k-space as far as q_c is of the order of the size of the Brillouin zone. The choice of a hyperbolic band allows us to carry out the calculation and to obtain an explicit expression for the imaginary part of Σ, which would not have been possible had we considered the original band (2). For the sake of brevity we just show how to proceed in the case $\varepsilon > 0$ to point out the effects that the introduction of a finite cut-off has on the self-energy. We insert the explicit expression of the band (5) in (6) and we operate the following substitutions: $x_k = k_x/\sqrt{2m_x}$, $y_k = k_y/\sqrt{2m_y}$, $x_c = q_c/\sqrt{2m_x}$, $y_c = q_c/\sqrt{2m_y}$, $x = x_k + q_x/\sqrt{2m_x}$ and $y = y_k + q_y/\sqrt{2m_y}$. Changing from the discrete sum to the integral in (6) we obtain

$$-\Im\Sigma(\underline{k}, \varepsilon) = \frac{g^2}{2\pi} \sqrt{m_x m_y} \int_{x_k - x_c}^{x_k + x_c} \mathrm{d}x \int_{y_k - y_c}^{y_k + y_c} \mathrm{d}y \; \delta(\varepsilon - \omega_0 - E_0 - x^2 + y^2) \tag{7}$$

where the ϑ function has been omitted provided that we impose the condition $\varepsilon > 0$. From (7) one may see that a finite cut-off introduces a dependence on $\underline{k}$ through the integral end points. Moreover a minimum and a maximum frequency are generated both in the positive and in the negative part of the quasi-particle spectrum, below the threshold at $-\omega_0$ and above the threshold at $+\omega_0$. These frequencies are determined by the zero-points in the argument of the δ function, that is present in (6) as well as the ϑ function. These zero-points must fall inside the range of integration in (7) so that kinematic bounds are generated on ε, defining a finite range of frequencies where $\Im\Sigma \neq 0$.

Indeed a reduction of the phononic phase space, produced by the introduction of a finite cut-off, provides further limits on the frequencies allowed in scattering processes so

that by decreasing q_c, the region where $\Im\Sigma \neq 0$ gets narrower. This may have important consequences on the quasi-particle spectrum, as even the discontinuities $\Im\Sigma$ shows at $\pm\omega_0$ can be eliminated by a reduction on q_c. This happens when the lowest positive (highest negative) frequency, generated in the spectrum by the δ function in (7), is higher (lower) than ω_0 ($-\omega_0$), defining a new threshold for the scattering; in this case $\Im\Sigma$ starts with continuity from the new threshold and the mass-anisotropy enhancement is not sizeable.

We have calculated the real part of the self-energy through a numerical Kramers–Krönig transformation on $\Im\Sigma$, which is nonzero in a finite range of energies. This has allowed us to obtain values for the spectral density, that is the distribution of the quasi-particle energies

$$A(\underline{k}, \varepsilon) = \frac{1}{\pi} \frac{|\Im\Sigma(\underline{k}, \varepsilon)|}{[\varepsilon - \xi(\underline{k}) - \Re\Sigma(\underline{k}, \varepsilon)]^2 + [\Im\Sigma(\underline{k}, \varepsilon)]^2} \tag{8}$$

if $\Im\Sigma \neq 0$ and

$$A(\underline{k}, \varepsilon) = \delta(\varepsilon - \xi(\underline{k}) - \Re\Sigma(\underline{k}, \varepsilon)) \tag{9}$$

if $\Im\Sigma = 0$. To carry on our calculation and get numerical results we have chosen the different parameters to obtain $\lambda \leqslant 1$ in (4) and a large value for q_c to focus on band-structure effects only, without including the effects associated to a reduction of the phase space allowed for scattering. Moreover we take $E_0 \simeq -56$ meV, $m_y \simeq 3.75 \times 10^{-3}$ meV^{-1}, $m_x \simeq r m_y$ with $r = 0.5$, $k_F \simeq 0.46$ with $E_0 + k_F^2/2m_x = 0$, $g \simeq 200$ meV, $\omega_0 \simeq 20$ meV, $q_c = 1$ or π.

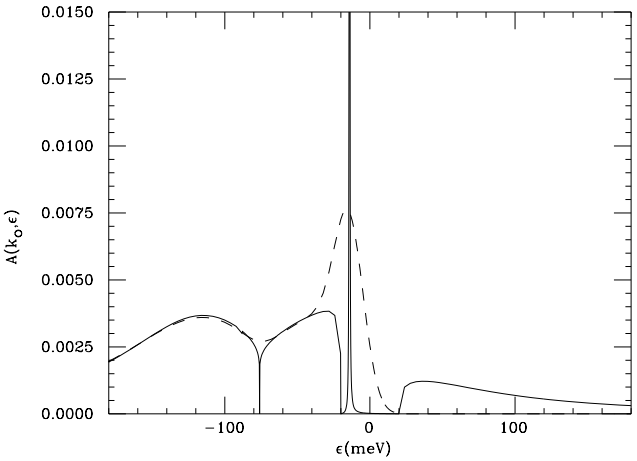

Figure 1. $A(\underline{k}, \varepsilon)$ at $\underline{k} = (0, \pi)$; the sharp Lorentzian peak located at the renormalized VHS energy $\tilde{E}_0 = -14.6$ meV is obtained by broadening the original δ function with a small imaginary part $\delta \sim 0.1$ meV whenever $\Im\Sigma = 0$; the dip in the continuous spectrum is due to a logarithmic singularity of $\Im\Sigma$ at $\varepsilon = -\omega_0 + E_0$. The dashed line represents the spectrum after the convolution with a Gaussian distribution of width 10 meV and the Fermi function at a temperature $T = 15$ K, to simulate typical experimental conditions.

The choice of a hyperbolic band, characterized by a VHS in the DOS $N(\varepsilon)$ at the energy E_0, does not allow for the approximation $N(\varepsilon) \simeq N(0)$ which was used to obtain a self-consistent, explicit expression of the self-energy for the parabolic band [9], and which, in that case, makes $\Im\Sigma$ symmetric for $\varepsilon \to -\varepsilon$; in the case of the bare electronic band (5) a different procedure is needed even to calculate the second-order diagram because of the strongly variable DOS. Moreover the symmetry $\varepsilon \to -\varepsilon$ is lost and, indeed, $\Im\Sigma$ may be singular at the energy $-\omega_0 + E_0$.

We have studied the spectral densities letting $\underline{k}$ vary in the x and in the y direction around the saddle point $(0, \pi)$, with the same procedure used in ARPES experiments [4, 5, 6, 7]. The δ function peak is at an energy of -14.6 meV in $(0, \pi)$ (see figure 1), thus fixing the position of the renormalized VHS; this peak moves left or right from this energy when $\underline{k}$ varies along the y or along the x direction starting from $(0, \pi)$.

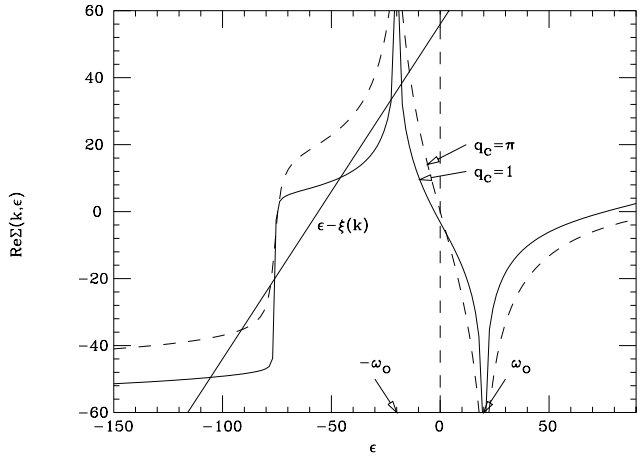

Figure 2. Real part of the self-energy, plotted both in the case $q_c = 1$ (full curve) and in the case $q_c = \pi$ (dashed curve); the intersection with the line $\varepsilon - \xi(\underline{k})$ gives the positions of the δ function peak and the broad features in figure 1. The dashed vertical line indicates the Fermi level.

A strong anisotropic mass enhancement is obtained, as the real part of the self-energy diverges at $\pm\omega_0$ (see figure 2). Indeed when $\underline{k}$ varies along the y direction, the intersection of the line $\varepsilon - \xi(\underline{k})$ with the curve $\Re\Sigma(\underline{k}, \varepsilon)$, which determines the position of the δ function peak (9), moves towards the singularity, and becomes pinned (see figure 2), producing an enhancement of the effective mass; however, when $\underline{k}$ varies along the x direction the peak moves towards the Fermi level, where the slope of the curve $\Re\Sigma$ is reduced (figure 2), so that the resulting effective mass is less enhanced.

We point out that the broad peak observed at an energy $\simeq -100$ meV in figure 1 results from the corresponding intersection of the line $\varepsilon - \xi(\underline{k})$ with the curve $\Re\Sigma(\underline{k}, \varepsilon)$ (see figure 2). To understand the presence of this feature one has to observe that $\Im\Sigma$ has a divergence at $-\omega_0 + E_0$, so that $\Re\Sigma$ has a jump at the same energy and is approximately flat above and below the jump. A quasi-particle peak may then appear at energies $\leqslant -\omega_0 + E_0$. This peak is, however, very broad, because of the large value of $\Im\Sigma$ close to the divergence, so that its position changes only slightly with varying $\underline{k}$.

In figure 3 we have plotted the position in energy of the δ peak for values of $\underline{k}$ where it fairly represents the electronic quasi-particle; interpolating the curves with parabolas we have obtained the new effective masses $m_y^* \simeq 29.0 \times 10^{-3}$ meV$^{-1} \simeq 7.7 m_y$, $m_x^* \simeq 7.7 \times 10^{-3}$ meV$^{-1} \simeq 4.1 m_x$, $m_y^*/m_x^* \simeq 3.76 \simeq 1.88\, m_y/m_x$. The ratio between the effective masses has an increase of 88% compared to the bare one; this indicates an increase in the anisotropy of the band. We have considered the effect of a reduction of q_c on the anisotropy of the mass renormalization repeating the same study in the case $q_c = 1$; this value of the cut-off is large enough to keep the dependence of the self-energy on $\underline{k}$ negligible in a wide region around the saddle point. Moreover a reduction of the phase space available for the scattering increases the spectral weight of the δ function compared to the continuous

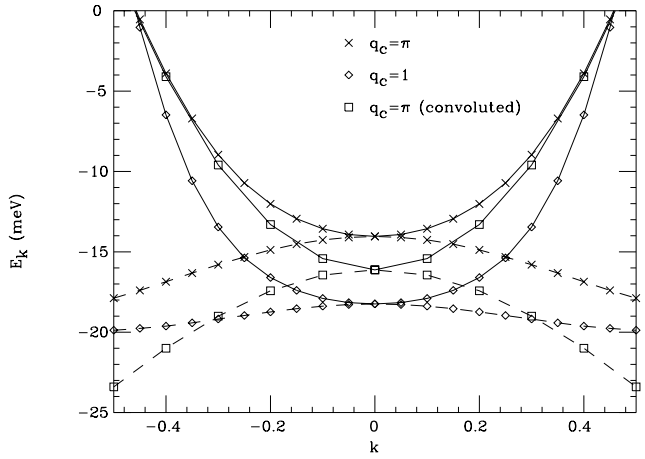

Figure 3. Quasi-particle bands obtained plotting the position of the δ function when $\underline{k}$ varies along the x (full curves) and y (dashed curves) directions, both in the case $q_c = \pi$ and in the case $q_c = 1$; a reduction of q_c increases the anisotropy of the band. We also show the renormalized bands after the convolution (10), in the case $q_c = \pi$, to point out how this operation does not eliminate the anisotropy of the band.

spectrum. We obtain $m_y^* \simeq 40.0 \times 10^{-3}$ meV$^{-1} \simeq 10.67 m_y$, $m_x^* \simeq 6.5 \times 10^{-3}$ meV$^{-1} \simeq 3.47 m_x$, $m_y^*/m_x^* \simeq 6.15 \simeq 3.08\ m_y/m_x$, and the energy for the VHS at $(0, \pi)$ is -18.2 meV. Thus, in the large-cut-off regime, a reduction of q_c increases the mass anisotropy. In figure 3 the renormalized bands are shown both in the case $q_c = \pi$ and in the case $q_c = 1$.

To make an easier comparison with the ARPES spectra [4–7] we have tried to simulate the experimental resolution (10 meV at best in [4]) and the effects of a finite temperature operating a convolution of our spectral densities with a Gaussian distribution weighted by the Fermi function

$$I(\underline{k}, \varepsilon) = \int_{-\infty}^{+\infty} \mathrm{d}\varepsilon' A(\underline{k}, \varepsilon') \frac{\mathrm{e}^{-(\varepsilon'-\varepsilon)^2/2\sigma^2}}{\sqrt{2\pi\sigma^2}} \frac{1}{\mathrm{e}^{\varepsilon'/KT} + 1} \tag{10}$$

where we have chosen $T = 15$ K and $\sigma = 10$ meV to reproduce the experimental conditions in [4]. The resulting intensity looks much more similar to the ARPES spectra as we show in figure 4; its energy varies between -15 and -25 meV when $\underline{k}$ varies along the y direction starting from $(0, \pi)$.

Moreover, although the peak now spreads over a larger range of energies, the anisotropy in the mass renormalization is not drastically reduced by the convolution. The new effective masses after the convolution are $m_y^* \simeq 16.0 \times 10^{-3}$ meV$^{-1} \simeq 4.27 m_y$, $m_x^* \simeq 6.5 \times 10^{-3}$ meV$^{-1} \simeq 3.47 m_x$, $m_y^*/m_x^* \simeq 2.46 \simeq 1.23\ m_y/m_x$. The effective-masses ratio has an increase of 23% compared to the bare one. The renormalized bands before and after the convolution are given in figure 3.

In conclusion we have shown that the electron–phonon interaction may produce a sizeable enhancement of mass anisotropy close to a saddle point. The effect is produced by different behaviour as the quasi-particle peak moves towards or away from the divergence in the real part of the self-energy. This mechanism is analogous to the one described in [9], where, however, an isotropic mass renormalization was found for the parabolic band. We point out that, even if the degree of anisotropy enhancement depends on the bare-mass ratio $(1 - \alpha)/(1 + \alpha)$, the mechanism described in this paper produces an anisotropy even

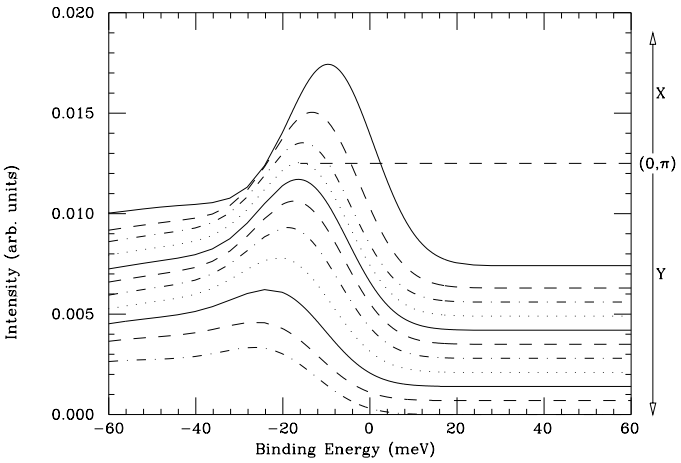

Figure 4. Spectra obtained from the convolution (10) plotted in sequence as $\underline{k}$ varies along the x and y directions starting from $(0, \pi)$. The position of the saddle point is indicated by the horizontal dashed line. The curves above (below) the curve at $\underline{k} = (0, \pi)$ are obtained by increasing k_x (decreasing k_y) of $\Delta k = 0.1$ for each curve.

at $\alpha = 0$, when the bare spectrum is isotropic around the saddle point. The relevant feature is indeed the presence of a VHS at an energy close to the phonon threshold $-\omega_0$.

The divergence of the density of states at the VHS, presumably limits our perturbative approach. The spirit of our calculation is, however, to choose the value of the electron–phonon coupling in such a way as to fulfil the weak-coupling condition close to the bottom of the band, where the density of states is slowly varying in two dimensions. In other words we compared the mass renormalization resulting from the second-order Fock diagram in two different regions of the electronic spectrum, to put in evidence the effect of a different form of the spectrum close to a saddle point. Other mechanisms for mass renormalization may arise as the strength of the electron–phonon interaction is increased towards the strong-coupling regime [11]. The analysis of the role of these strong-coupling polaronic effects, close to a saddle point, was however out of the scope of this paper.

Acknowledgments

We gratefully acknowledge useful discussions with C Di Castro, C Castellani and M Grilli. SC acknowledges financial support of the INFM, PRA 1996.

References

[1] Labbé J and Bok J 1987 *Europhys. Lett.* **3** 1225
Friedel J 1987 *J. Physique* **48** 1787
Dzyaloshinskiĭ I E 1987 *Sov. Phys.–JETP* **66** 848
[2] Newns D M, Tsuei C C, Pattnaik P C and Kane C L 1992 *Comment. Condens. Matter. Phys.* **15** 273
Tsuei C C, Newns D M, Chi C C and Pattnaik P C 1990 *Phys. Rev. Lett.* **65** 2724
[3] Van Hove l 1953 *Phys. Rev.* **89** 1189
[4] Gofron K, Campuzano J C, Abrikosov A A, Lindroos M, Bansil A, Ding H, Koelling D and Dabrowski B 1994 *Phys. Rev. Lett.* **73** 3302
[5] Abrikosov A A, Campuzano J C and Gofron K 1993 *Physica* C **214** 73
[6] Dessau D S *et al* 1993 *Phys. Rev. Lett.* **71** 2781

Jian Ma, Quitmann C, Kelley R J, Alméras P, Berger H, Margaritondo G and Onellion M 1995 *Phys. Rev.* B **51** 3832

[7] King D M, Shen Z-X, Dessau D S, Park C H, Spicer W E, Peng J L, Li Z Y and Greene R L 1994 *Phys. Rev. Lett.* **73** 3298

[8] Campuzano J C *et al* 1996 *Phys. Rev.* B **53** R14737
Norman M R, Ding H, Campuzano J C, Takeuchi T, Randeria M, Yokoya T, Takahashi T, Mochiku T and Kadowaki K 1997 *Report No.* cond-mat/9702144

[9] Engelsberg S and Schrieffer J R 1963 *Phys. Rev.* **131** 993

[10] The issue of vertex corrections close to a VHS was addressed in: Cappelluti E and Pietronero L 1996 *Phys. Rev.* B **53** 932. The authors show in particular that in the adiabatic regime the validity of Migdal's theorem is not weakened due to the presence of a VHS, provided a suitable definition of the coupling constant λ is used.

[11] Aleksandrov A S, Grebenev V N and Mazur E A 1987 *Sov. Phys.– JETP Lett.* **45** 455